Timbral Coloration in High Resolution Sound Field Reproduction Due to Spatial Bandwidth Limitation

Jens Ahrens and Sascha Spors

Deutsche Telekom Laboratories, Technische Universität Berlin, Ernst-Reuter-Platz 7, 10587 Berlin, Germany

Introduction

Sound field reproduction methods based on orthogonal expansions like e.g. higher order Ambisonics always introduce a limitation of the spatial bandwidth of the loudspeaker driving signals. As a consequence, the desired component of the reproduced wave field is similarly bandlimited. This leads to a pronounced sweet spot around the center of the loudspeaker distribution. This area is sweet both in terms of spatial aliasing artifacts as well as in terms of accuracy of the desired component of the reproduced wave field. The sweet spot gets significantly smaller with increasing temporal frequency. This means that outside the center of the loudspeaker distribution, the point of most accurate reproduction, frequency dependent artifacts arise. In this paper, we objectively investigate the resulting artifacts for circular loudspeaker arrangements with a focus on potential consequences on human perception.

Theory

We briefly revisit the theory of sound field reproduction relevant to the presented investigation in this and the following two sections. Refer to [1, 2] for an extensive treatment.

The sample scenario under consideration in this paper is a virtual plane wave reproduced by a circular distribution of secondary line sources (i.e. purely 2D reproduction). The choice of a plane wave is justified since arbitrary propagating wave fields can be described by an appropriate superposition of plane waves [3].

The secondary line sources are positioned perpendicular to the target plane (the receiver plane). For convenience we specialize the formulation to this particular case. Our approach is therefore not directly implementable since loudspeakers exhibiting the properties of line sources are commonly not available. Real-world implementations usually employ loudspeakers with closed cabinets as secondary sources. The properties of these loudspeakers are more accurately modeled by point sources.

The main motivation to focus on two dimensions is to keep the mathematical formulation simple in order to illustrate the fundamental properties. The extension both to three-dimensional reproduction (i.e. spherical arrays of secondary point sources) and to two-dimensional reproduction employing circular arrangements of secondary point sources (*2½-dimensional reproduction*) is straightforward and a general treatment thereof can be found e.g. in [2, 4].

It can be shown that either of the established sound field reproduction methods (i.e. higher order Ambisonics and wave field synthesis) is capable of reproducing sound fields with limited spatial bandwidth [1]. However, wave field synthesis is typically implemented in the time domain. This approach is very efficient for certain spatially unlimited driving functions. Typically, for reproduction with limited spatial bandwidth, an Ambisonics-related approach is used. For convenience, we follow this practice and consider an Ambisonics-like approach in the remainder of this paper.

The Ambisonics-Like Approach

In this section, we briefly review an approach for spatially bandlimited reproduction which is typically associated with near-field compensated higher order Ambisonics. In the remainder of this paper, we call this approach *Ambisonics-like* and not *Ambisonics* since the term Ambisonics (and also near-field compensated higher order Ambisonics) refers to a specific approach which has evolved over many years and whose nomenclature is not perfectly in line with the presented approach (compare e.g. to [5]). The formulation treated in this section has been presented by the authors in [1, 2]. Its physical fundament is the so-called *simple source approach*. The simple source approach for interior problems states that the acoustic field generated by events outside a volume can also be generated by a continuous distribution of secondary simple sources enclosing the respective volume [3].

The reproduction equation for a continuous circular distribution of secondary line sources and with radius r_0 centered around the origin of the coordinate system is then given by [1]

$$P(\mathbf{x},\omega) = \int_0^{2\pi} D(\alpha_0,\omega)\ G_{2\mathrm{D}}(\mathbf{x}-\mathbf{x}_0,\omega)\ r_0\ d\alpha_0\ , \quad (1)$$

where $\mathbf{x}_0 = r_0 \cdot [\cos\alpha_0\ \ \sin\alpha_0]^T$. $P(\mathbf{x},\omega)$ denotes the reproduced wave field, $D(\alpha_0,\omega)$ the driving function for the secondary source situated at $\mathbf{x}_0$, and $G_{2\mathrm{D}}(\mathbf{x}-\mathbf{x}_0,\omega)$ its two-dimensional spatio-temporal transfer function.

A fundamental property of (1) is its inherent non-uniqueness and ill-posedness [6]. I.e. in certain situations, the solution is undefined and so-called *critical* or *forbidden frequencies* arise. The forbidden frequencies represent the resonances of the cavity under consideration. However, there are indications that the forbidden frequencies are only of minor relevance when practical implementations are considered [3, 2].

Equation (1) constitutes a circular convolution and therefore the convolution theorem

$$\mathring{P}_\nu(r,\omega) = 2\pi r_0\ \mathring{D}_\nu(\omega)\ \mathring{G}_\nu(r,\omega) \quad (2)$$

applies [7]. $\mathring{P}_\nu(r,\omega)$, $\mathring{D}_\nu(\omega)$, and $\mathring{G}_\nu(r,\omega)$ denote the Fourier series expansion coefficients of $P(\mathbf{x},\omega)$, $D(\alpha,\omega)$, and $G_{\mathrm{2D}}\left(\mathbf{x}-[r_0\ 0]^T\right)$[1].

Equation (2) can be solved for $\mathring{D}_\nu(\omega)$. The secondary source driving function $D(\alpha_0,\omega)$ for a secondary source situated at position $\mathbf{x}_0$ reproducing a desired wave field with expansion coefficients $\breve{P}_\nu(\omega)$ can then be determined as [1]

$$D(\alpha,\omega) = \frac{1}{2\pi r_0} \sum_{\nu=-\infty}^{\infty} \frac{\breve{P}_\nu(\omega)}{\breve{G}_\nu(\omega)} e^{j\nu\alpha} \ , \qquad (3)$$

whereby we omitted the index 0 in α_0 for convenience. Note that $D(\alpha,\omega)$ is independent from the receiver position. The coefficients $\breve{F}_\nu(\omega)$ of a function $F(\mathbf{x},\omega)$ are defined via

$$F(\mathbf{x},\omega) = \sum_{\nu=-\infty}^{\infty} \underbrace{\breve{F}_\nu(\omega) J_\nu\left(\frac{\omega}{c}r\right)}_{\mathring{F}_\nu(\omega,r)} e^{j\nu\alpha} \ , \qquad (4)$$

whereby $J_\nu(\cdot)$ denotes the ν-th order Bessel function [3]. Refer to [1] for the explicit driving function for the considered scenario of a virtual plane wave reproduced by a circular distribution of secondary line sources.

The driving function (3) is not per se spatially bandlimited (ν can take any integer value). However, (3) straightforwardly allows to apply a spatial bandlimitation (refer also to the following section). In the latter case, the summation over ν is only performed between the limits $-N$ and N. One then speaks of a spatial bandwidth of N respectively of N-th order reproduction.

Spatial discretization

For the theoretic continuous secondary source distribution, any wave field which is source-free inside the secondary source distribution can be accurately reproduced apart from the forbidden frequencies. Real-world implementations of audio reproduction systems always employ a finite number of discrete secondary sources. This spatial discretization can result in spatial aliasing. In this section, we briefly review the consequences of spatial discretization. A thorough treatment can be found in [1, 2].

It can be shown that the angular sampling of the driving function results in repetitions of the angular spectrum (i.e. in the present case the Fourier expansion coefficients $\mathring{D}_\nu(\omega)$) of the continuous driving function $D(\alpha,\omega)$

$$\mathring{D}_{\nu,S}(\omega) = \sum_{\eta=-\infty}^{\infty} \mathring{D}_{\nu+\eta L}(\omega) \ , \qquad (5)$$

when L equiangular sampling points (i.e. loudspeakers) are taken. Equation (2) states that the angular spectrum of the reproduced wave field $\mathring{P}_\nu(r,\omega)$ is equal to the angular spectrum of the driving function $\mathring{D}_\nu(\omega)$ weighted by the angular spectrum of the secondary sources $\mathring{G}_\nu(r,\omega)$. Note that all angular spectra are taken with respect to the expansion around the origin of the global coordinate system.

In order to yield the angular spectrum $\mathring{P}_{\nu,S}(r,\omega)$ of the wave field reproduced by a discrete secondary source distribution, the spectral repetitions given by (5) have to be introduced into (2). The case of $\eta = 0$ then describes the desired component of the reproduced wave field. In other words: Despite sampling the desired component of the reproduced wave field is always present. The cases of $\eta \neq 0$ describe additional components due to sampling. These additional components can not be avoided.

As stated in the previous section, the driving function (3) is not per se bandlimited with respect to the angular frequency ν. Thus, when the angular bandwidth of the driving function is not artificially limited, the angular repetitions overlap and interfere.

In order to avoid such overlapping and interference of the spectral repetitions, the angular bandwidth of the continuous driving function of the Ambisonics-like approach (3) can be limited as

$$D_N(\alpha,\omega) = \frac{1}{2\pi r_0} \sum_{\nu=-N}^{N} \frac{\breve{P}_\nu(\omega)}{\breve{G}_\nu(\omega)} e^{j\nu\alpha} \ , \qquad (6)$$

whereby $N = \frac{L-1}{2}$ when a discrete distribution of an odd number L of secondary sources is considered and accordingly for even L. Strictly spoken, when (6) is applied spatial aliasing is prevented in the driving function since no spectral overlaps occur. However, since the spatial spectrum $\mathring{G}_\nu(r,\omega)$ of the secondary sources is not bandlimited, spatial repetitions of the driving function are always reproduced. Although this is rather a reconstruction error [1] it is commonly also referred to as spatial aliasing. We do so as well in the remainder for convenience. Note that it is actually impossible to implement the Ambisonics-like approach (3) with infinite bandwidth since this would require an infinite summation.

Continuous Secondary Source Arrays

At a first stage, we consider the reproduction via continuous secondary source distributions. These provide reproduction which is perfectly free of spatial discretization artifacts. They therefore allow to independently investigate the properties of the desired component of the reproduced wave field. For convenience, we consider a virtual plane wave as desired wave field to be reproduced. It can be shown that continuous secondary source distributions reproduce a wave field with exactly the same spatial bandwidth like the driving function [1, 2]. Refer to figure 1 for an illustration of the general properties. The most important of which are summarized in the following list:

- For low frequencies, the reproduction is almost perfect (refer to figure 1(a)).
- For higher frequencies, the energy of the reproduced wave field concentrates around the center of the

[1] Note that the coefficients $\mathring{G}_\nu(r,\omega)$ as used throughout this paper assume that the secondary source is situated at the position $(r = r_0, \alpha = 0)$ and is orientated towards the coordinate origin.

secondary source distribution (refer to figure 1(b)). This is a direct consequence of the spatial bandwidth limitation and is reflected by the properties of the involved Bessel functions. This concentration of the energy around the center of the secondary source distribution is more pronounced the higher the temporal frequency. In other words, for receiver positions outside the center, high frequencies are significantly attenuated (by several dB). Therefore, timbral coloration might occur.

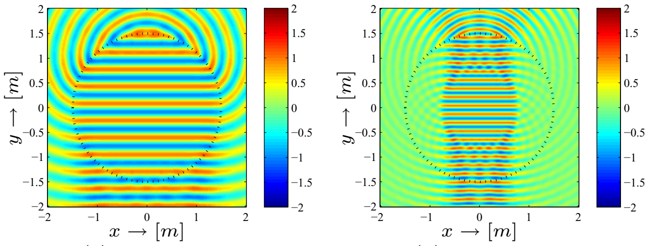

(a) $f = 1000$ Hz. (b) $f = 2000$ Hz.

Figure 1: $\Re\{P(\mathbf{x}, \omega)\}$ of a continuous secondary source distribution with $r_0 = 1.5$ m reproducing a plane wave of different temporal frequencies. A spatial bandwidth limitation of $N = 27$ is applied.

Discrete Secondary Source Arrays

In this section, we move further to discrete secondary source distributions. This is what we find in real-world implementations. Again, we consider a virtual plane wave as desired wave field to be reproduced.

Below a certain critical frequency which we term *spatial aliasing frequency* the ratio of the energy of spatial discretization artifacts and the energy of the desired component of the reproduced wave field is very low and the reproduction is considered aliasing-free. Above the spatial aliasing frequency, the above described energy ratio rises quickly and reproduction is considered being corrupted by spatial aliasing [1].

The artifacts which arise due to the spatial discretization are superposed to those artifacts due to spatial bandwidth limitation. The properties of the discretization artifacts are strongly related to the spatial bandwidth of the driving function and can therefore not be treated independently.

The general properties of discrete secondary source distributions driven with finite spatial bandwidth signals can be deduced from figure 2 and are summarized in the following list:

- The center of the secondary source distribution stays essentially free of aliasing artifacts. The higher is the frequency, the smaller is this sweet area.
- Outside the sweet area, strong aliasing artifacts arise.
- The energy of the aliasing artifacts is not equally distributed over the receiver area. I.e., the energy of the artifacts is strongly dependent on the position. This indicates that also the perception is strongly dependent on the listener position.
- The spatial structure of the aliasing artifacts is quite regular. The latter can locally be interpreted as plane wave fronts originating from that point on the secondary source contour where the desired virtual plane wave arrives. This could result in a localization bias and impair the localization quality of the virtual source. Refer to section *Localization* for a further discussion.

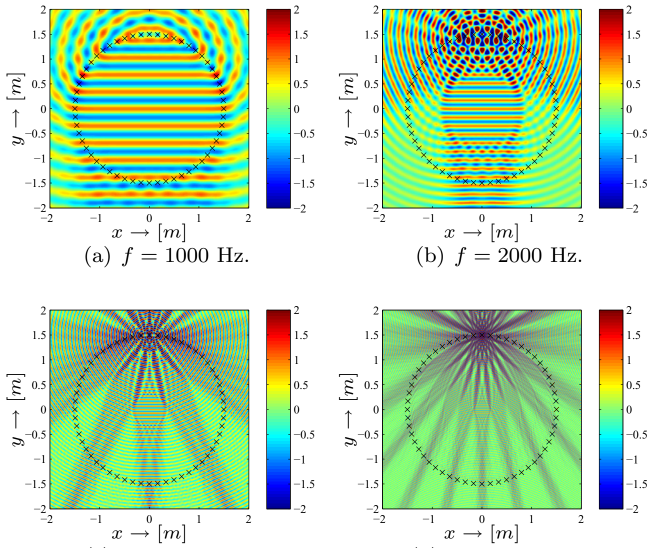

(a) $f = 1000$ Hz. (b) $f = 2000$ Hz.

(c) $f = 5000$ Hz. (d) $f = 10000$ Hz.

Figure 2: $\Re\{P(\mathbf{x}, \omega)\}$ of a discrete secondary source distribution with $r_0 = 1.5$ m reproducing a plane wave of different temporal frequencies. A spatial bandwidth limitation of $N = 27$ is applied.

Transfer Function of Discrete Secondary Source Distributions

In order to get more insight into the consequences of the different energy distributions in the receiver area, we present the transfer function of the discrete secondary source distribution under consideration. As in the previous sections, the desired wave field to be reproduced is a plane wave.

Figures 3(a) and 3(b) illustrate the global variation of the absolute value of the transfer function between the secondary source distribution and selected receiver positions, i.e. we investigate a selection of receiver points which are distributed over the entire receiver area.

Figures 3(c) and 3(d) illustrate the local variation of the absolute value of the transfer function, i.e. we investigate a selection of receiver points which are located within the vicinity of each other.

- A sweet spot with perfectly flat frequency response is apparent in the center of the secondary source distribution (refer to the black line in figures 3(a) and 3(b)).
- Obvious variations of the absolute value of the transfer function arise above the aliasing frequency

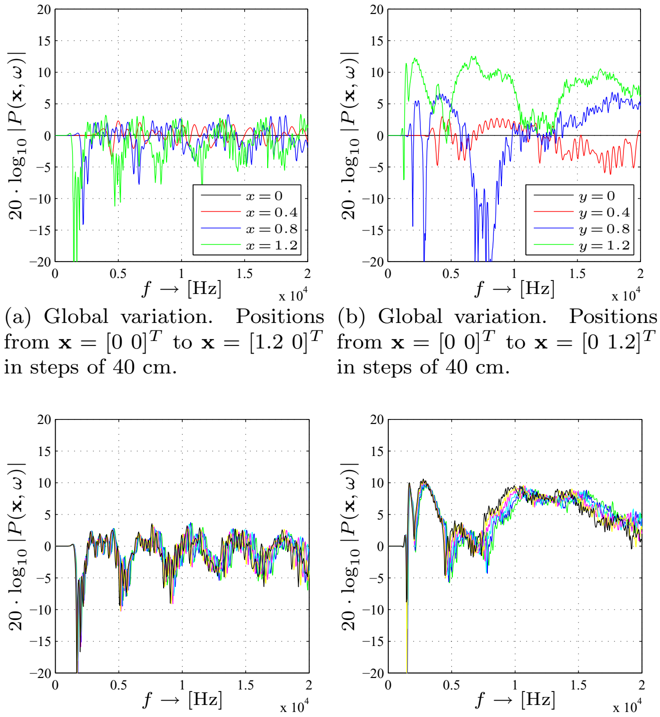

(a) Global variation. Positions from $\mathbf{x} = [0\ 0]^T$ to $\mathbf{x} = [1.2\ 0]^T$ in steps of 40 cm.

(b) Global variation. Positions from $\mathbf{x} = [0\ 0]^T$ to $\mathbf{x} = [0\ 1.2]^T$ in steps of 40 cm.

(c) Local variation. Positions from $\mathbf{x} = [1\ 0]^T$ to $\mathbf{x} = [1.05\ 0]^T$ in steps of 1 cm.

(d) Local variation. Positions from $\mathbf{x} = [0\ 1]^T$ to $\mathbf{x} = [1\ 1.05]^T$ in steps of 1 cm.

Figure 3: Variations of the absolute value of the temporal transfer function of a discrete secondary source distribution with $r_0 = 1.5$ m to selected receiver positions. Spatial bandwidth limitation applied ($N = 27$).

for positions along the x-axis (refer to figure 3(a)).

- For positions along the y-axis strong variations arise (refer to figure 3(b)).
- Only minor variation is apparent when moving around a selected position on the x-axis (refer to figure 3(c)). The general properties of the transfer function stay similar.
- The same holds true for the vicinity of a position on the y-axis (refer to figure 3(d)). In this case the deviation from the desired flat frequency response is significantly stronger than for lateral positions.
- Below the aliasing frequency (which varies strongly with the receiver position), the transfer function is perfectly flat.

Localization

As can be seen from figures 2(c) and 2(d), the spatial aliasing artifacts have a regular spatial structure. Locally, the spatial aliasing artifacts can be interpreted as plane wave fronts originating from that point on the secondary source contour where the virtual plane wave front first hits the secondary source contour. As a consequence, listeners positioned outside the sweet area (the latter being almost aliasing-free) might localize the high-frequency content above the spatial aliasing frequency at the above mentioned position on the secondary source contour. The low-frequency content below the spatial aliasing frequency is localized in the direction where the plane wave comes from. Note that there is no smooth transition between the two perceived source locations. Informal listening suggests that it might also happen that two individual virtual sources are perceived.

Conclusions

We have presented simulations of wave fields reproduced by a circular array of loudspeakers. We focused on an investigation of the artifacts arising in the reproduction of finite spatial bandwidth. We chose an Ambisonics-like approach to represent this type of reproduction.

The major findings are: (1) A pronounced sweet spot arises in the center of the secondary source distribution. (2) The energy of spatial aliasing artifacts is heavily dependent on the position with only very little local variation.

Our simulations suggest that the properties of the aliasing artifacts are audible as timbral coloration and possibly also impairment of the localization quality of a virtual source. However, reliable conclusions can not be drawn from such simulations. A listening test to verify the results is in preparation.

An investigation of the properties of infinite spatial bandwidth sound field reproduction as it typically occurs in wave field synthesis can be found in [8].

References

[1] S. Spors and J. Ahrens. A comparison of wave field synthesis and higher-order Ambisonics with respect to physical properties and spatial sampling. In *125th Conv. of the AES*, San Francisco, CA, Oct. 2–5 2008.

[2] J. Ahrens and S. Spors. An analytical approach to sound field reproduction using circular and spherical loudspeaker distributions. *Acta Acustica utd. with Acustica*, 94(6):988–999, Nov./Dec. 2008.

[3] E. G. Williams. *Fourier Acoustics: Sound Radiation and Nearfield Acoustic Holography*. Academic Press, London, 1999.

[4] S. Spors, R. Rabenstein, and J. Ahrens. The theory of wave field synthesis revisited. In *124th Convention of the AES*, Amsterdam, The Netherlands, May 17–20 2008.

[5] J. Daniel. Représentation de champs acoustiques, application à la transmission et à la reproduction de scènes sonores complexes dans un contexte multimédia. PhD thesis Université Paris 6, 2001.

[6] L. G. Copley. Fundamental results concerning integral representations in acoustic radiation. *JASA*, 44:28—-32, 1968.

[7] B. Girod, R. Rabenstein, and A. Stenger. *Signals and Systems*. J.Wiley & Sons, 2001.

[8] J. Ahrens and S. Spors. Alterations of the temporal spectrum in high-resolution sound field reproduction of varying spatial bandwidths. In *126th Conv. of the AES*, Munich, Germany, May. 7–10 2009.